Nanoplasma-based Millimiter-wave Modulators on a Single Metal Layer

Mohammad Samizadeh Nikoo, Majid Olad Dilmaghanian, Forouhar Farzaneh, *Senior Member, IEEE,* and Elison Matioli, *Senior Member, IEEE*

***Abstract*—Fundamental constraints imposing power-frequency trade-offs in conventional electronics have stimulated research on alternative technologies for millimeter-wave and sub-millimeter-wave applications. In this work, we use the picosecond threshold firing of nanoplasma switches to demonstrate on-chip millimeter-wave modulators that rely on a single metal layer. We show amplitude shift keying (ASK) modulation with self-synthesized carrier frequencies up to 66 GHz (limited by the bandwidth of our experimental setup), with output power of 30 dBm. These all-metal nanoplasma modulators are low cost, and generally compatible with different platforms, from CMOS and III-V compounds to flexible substrates. Our work paves the way towards future terahertz communication circuits with large output powers, which otherwise are not practical using high-power amplifiers at frequencies over 100 GHz. In a more general context, the proposed all-metal circuits can potentially synthesize arbitrarily-shaped ultra-wide-band (UWB) signals with applications in advanced wireless communications, radars, and imaging systems.**

***Index Terms*—Millimeter-wave, terahertz, ASK, modulators, nanoplasma switch, all-metal circuits.**

I. Introduction

SYNTHESIZING and amplifying millimeter-wave (mm-wave) and terahertz signals are challenging in traditional semiconductor electronics [1], [2]. As the dimensions of metal-oxide-semiconductor (MOS) devices are reduced to achieve higher cut-off frequencies, their delivered power drastically decreases [3]. For narrow-band systems, including different types of modulators, the classic approach is to use a microwave local oscillator followed by a power amplifier which drives a chain of frequency multipliers [4]. This results in a rather low-power signal at millimeter or sub-millimeter bands that is delivered to a modulating switch [5] whose cut-off frequency limits the maximum operation frequency of the system.

Such technical challenges are more severe for RF systems that require ultra-wide-band (UWB) signals [6], [7]. Digital approaches to synthesize rich-frequency waveforms are bulky and quite limited in terms of bandwidth. Power amplification of such wide-band signals is also very difficult. Alternative analog approaches have been explored to directly generate UWB signals, like impulses [8]. Ultrafast reverse recovery of p-i-n diodes [9] and nonlinear wave-lattice interactions [10] that produces self-compressed electrical pulses [11] are examples of such alternative techniques. Besides the relatively low output power of these approaches, the requirement for specific semiconductor epitaxies can hinder their application in conventional integrated circuits.

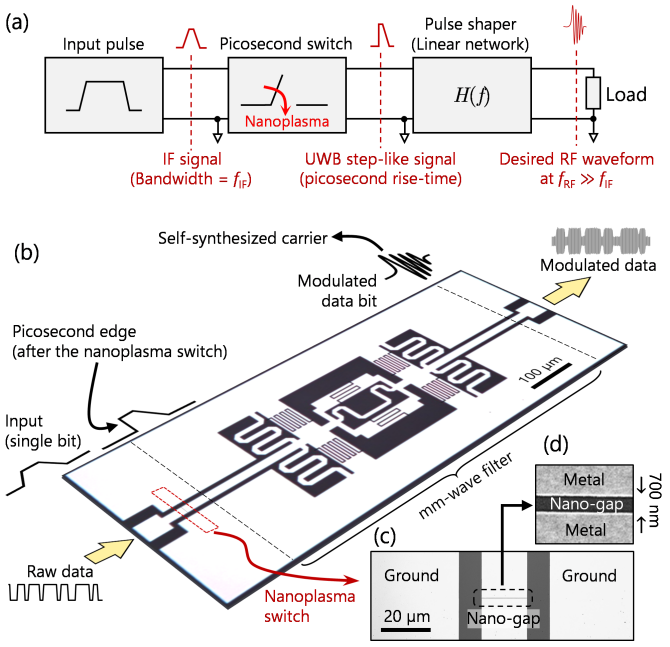

Fig. 1. (a) Schematic of the proposed analog synthesizer based on a picosecond threshold-firing switch (nanoplasma device). (b) Nanoplasma-based single-metal-layer modulator. The figure illustrates the perspective optical microscope picture of a fabricated modulator. The structure is driven by a sequence of data bits. Data bits corresponding to "1", trigger the nanoplasma device which generates a step-like UWB signal. The UWB signal passes through a coplanar filter that transfers the step-like shape to a wave-packet with the desired frequency content. (c) Scanning electron microscope (SEM) image of a nanoplasma device integrated on a coplanar waveguide. (d) SEM image of the nano-gap.

Here we propose to use the picosecond threshold firing in recently demonstrated nanoplasma devices [3], integrated with a coplanar patterned metal layer, to generate and modulate mm-wave and terahertz signals at large power levels. As shown in Fig. 1a, an ordinary source (which can have a low bandwidth in the range of MHz) injects a pulse to a nanoplasma switch. The switch transfers the input pulse into a signal with a picosecond rise-time which has an ultra-wide bandwidth up to the THz band [3]. This UWB signal passes through a linear network (transfer function H) which shapes it into the desired waveform at the output load. In the case of H being a band-

M. Samizadeh Nikoo and E. Matioli are with the Power and Wide-band-gap Electronics Research Laboratory (POWERlab), École polytechnique fédérale de Lausanne (EPFL), CH-1015 Lausanne, Switzerland (mohammad.samizadeh@epfl.ch, elison.matioli@epfl.ch).

M. Olad Dilmaghanian and F. Farzaneh are with the Department of Electrical Engineering, Sharif University of Technology, Tehran, Iran.

Manuscript received February 22, 2022.

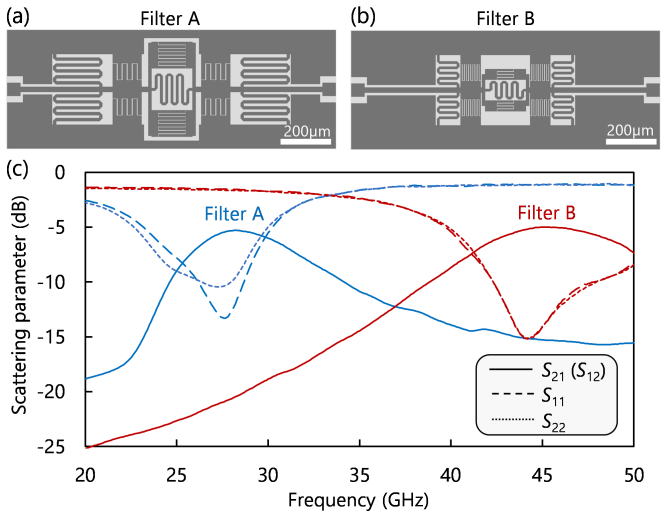

Fig. 2. (a) Layouts of filters (a) A, and (b) B. The darker color represents the metallic region. (c) On-wafer scattering parameter characterization of two fabricated bandpass filters designed with central frequencies of 28 GHz (filter A) and 45 GHz (filter B) using a 50-GHz vector network analyzer (VNA). Transmission (S12 = S12) shown by solid lines and reflection (S11 and S22) shown by dashed lines.

pass filter, the output pulse is a wave-packet, and the entire structure acts an amplitude-shift keying self-modulator.

This concept relies on a single metal layer (Fig. 1b), and integrates several functions together, enabling a simple, compact and low-cost digital data modulator in the millimeter and terahertz bands. The proposed all-metal circuits (in the form of two-port networks) consist of two parts: 1. A nanoplasma switch right after the input port of the network (Fig. 1c-d), and 2. A linear coplanar network with a designed transfer function H(f) which shapes the signal generated by the nanoplasma switch.

Nanoplasma device is capable of switching signals with amplitudes from a few volts to thousands of volts [3], [12]. Therefore, the proposed concept can provide a wide range of power levels from milliwatts to kilowatts. Recombination rates of less than 20 ns (limited by the experimental setup) have been demonstrated for nanoplasma switches [3], which can enable high data rates over 100 Mb/s.

II. Experiments and Results

The nanoplasma-based modulators were fabricated on a 2- inch sapphire substrate. The process flow started with a metal deposition step (500 nm-thin Au, along with 3-nm thin Cr adhesion layers). Nano-gaps were patterned by e-beam lithography (using ZEP positive resist) followed by ion-beam etching. Coplanar filters were then defined by photolithography, followed by an ion-beam etching step. We characterized the all-metal modulators designed with four different bandpass filters, named filters A, B, C, and D with central frequencies at 28 GHz, 45 GHz, 55 GHz, and 65 GHz, respectively, each of them including three series of coplanar resonators. Figs. 2a and 2b illustrate layouts of filters A and B, respectively. The detailed design of all filters is presented in the supplementary document. Fig. 2c shows the

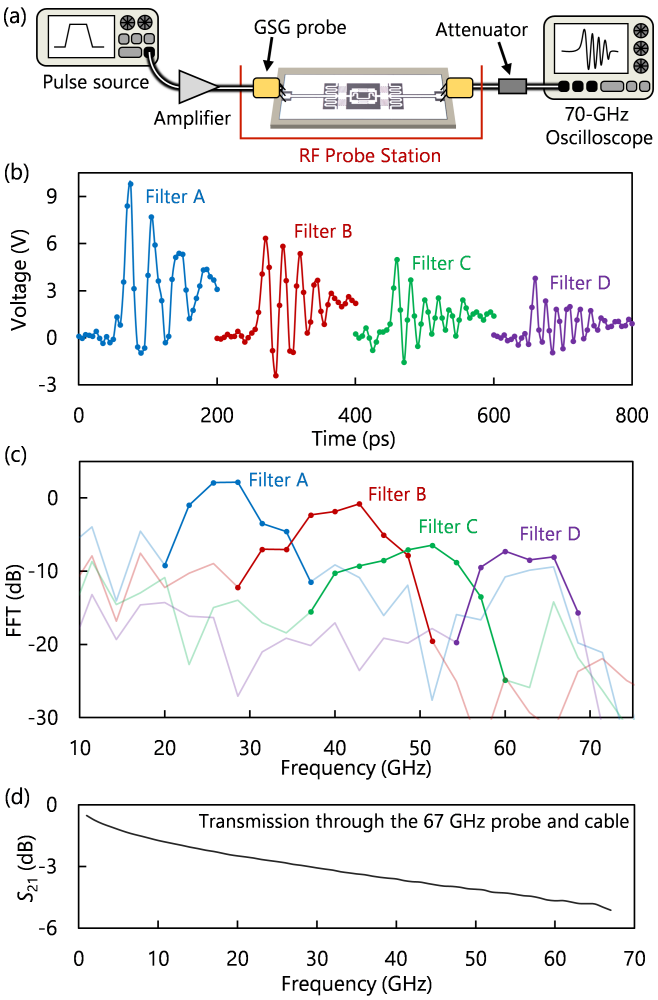

Fig. 3. (a) Schematic of the experimental setup. A function generator with an IF amplifier stage drives the all-metal modulator terminated by a 70-GHz oscilloscope. The input and output ports of the modulator were accessed through 67-GHz ground-signal-ground (GSG) RF probes. (b) Output voltage of the all-metal modulators with four different filters, designed at 28 GHz, 45 GHz, 55 GHz, and 66 GHz. The points correspond to the digital sampling of the oscilloscope. (c) FFT of the captured waveforms. (d) Transmission scattering parameter through the probe and the cable, reported by the datasheets.

measured reflection (dashed lines) and transmission (solid lines) of the fabricated filters with central frequencies of 28 GHz (filter A, blue lines) and 45 GHz (filter B, red lines). For the scattering parameter characterizations, our measurements were limited by the bandwidth of the 50-GHz performance network analyzer (PNA) (Keysight N5225A). The measurements were done on-wafer in which the two coplanar ports of the filters were connected to coaxial cables (terminated by two ports of the PNA) through 67-GHz ground-signal-ground (GSG) RF probes. The time-domain performance of the fabricated modulators was evaluated using a 70-GHz oscilloscope (DPO77002SX) with an ultrahigh sample rate of 200 GS/s (Fig. 3a). Electrical pulses generated by a function generator were amplified by an intermediate frequency (IF) amplifier with 5 MHz bandwidth and 34-dB gain to drive a 700-nm-long gap nanoplasma switch. The output port of

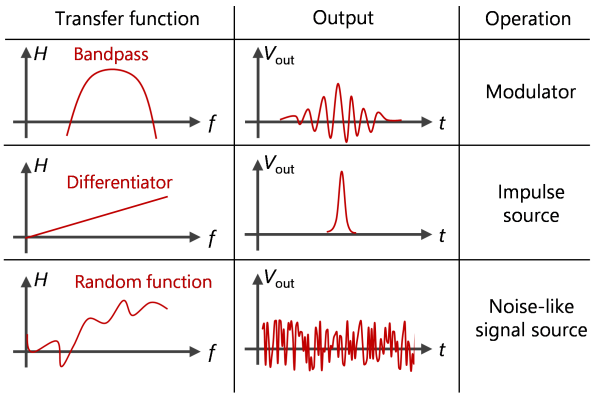

Fig. 4. Illustration of three examples of transfer functions and their corresponding output waveforms.

the modulator was accessed through a 67-GHz GSG probe connected to a 1.85-mm cable terminated to the 70-GHz port of the oscilloscope with an external 67-GHz 40-dB attenuator. The attenuator was used to downscale the modulated wave into the measurement range of the oscilloscope (350 mV peak-to-peak). Fig. 3b illustrates waveforms at the output port of the modulators, which correspond to the measured waveforms by the oscilloscope multiplied by 100 (to compensate for the 40-dB attenuation). The discrete points correspond to the samples taken by the oscilloscope with interval of 5 ps.

The output waveform shape and its frequency content are determined by the design of the coplanar filter. As shown in Fig. 3c, the central frequency of the output pulse can be shifted from 28 GHz to over 60 GHz by changing the layout design of the filter (which in this work was limited by our measurement equipment). The modulator provides a high output power level without an RF amplifier stage, which is one of the most costly and challenging parts of millimeter-wave communication systems. In fact, here there is only one IF amplifier to drive the nanoplasma device, which should only support the much lower bandwidth of the data-rate. The picosecond switching capability of the nanoplasma devices [3] can potentially enable modulation into the terahertz band, bridging the gap between RF and optical modulators [13]-[14].

The output power of the modulator becomes lower at higher frequencies (Fig. 3b), since the filter is excited by a step-like signal (Fig. 1), whose frequency content (FFT magnitude) is proportional to the inverse of frequency. This behavior is similar to the general power-frequency trade-off in RF sources (Pf2 = constant, where P and f represent the output power and frequency of the RF source) [3]. Despite this general trade-off, the output power of the proposed modulator is quite high. The output voltage level at the 50- load is in range of several volts, which considering the attenuation of the cable and probe (Fig. 3d), results in Watt-range power levels. The output power can be further increased by optimization of the designed filters, as they currently exhibit at least a 5 dB insertion loss at their central frequencies (Fig. 2c). Another way to adjust the output power is by changing the gap size of the nanoplasma device, which can tune its operation voltage in a very wide range, from a few volts to thousands of volts [12].

III. Discussions

From a more general point of view, the concept proposed can potentially enable synthesizing analog waveforms with designed shapes. This is challenging to do with classic digital sampling methods for two reasons. First, high-frequency signals require ultrahigh sampling rates, which is difficult at the millimeter and submillimeter bands. Second, the amplification of signals with a rich frequency content is a major challenge. For instance, the fast Fourier transform (FFT) of noise-like signals that are interesting for radar applications [15] can cover a wide range of frequencies, much larger than that achievable with UWB amplifiers [16]. Impulse waveforms are other sort of UWB signals with applications in communications [6], radars [17], imaging [18], and broad-band spectroscopy systems [19].

From a general point of view, Fig. 1a shows the block diagram of a universal nanoplasma-based analog synthesizer. A nanosecond pulse source, generated by an ordinary electronic circuit, drives a nanoplasma switch in series with a patterned coplanar structure with transfer function H. The amplitude and phase of H precisely controls the shape of the output signal delivered to the load, which can be a radiating element. Fig. 4 illustrates some possible transfer functions and the corresponding output signals, showing the potential functionality of the synthesizer. For a bandpass filter, as described in the previous section, the output signal is a wave-packet, and the system operates as a modulator.

Replacing the bandpass filter by a differentiator [20], the system can potentially generate impulse-like signals. The design of the differentiator determines the spectrum of the generated impulses. The nanoplasma devices offer switching times faster than 5 ps (limited by the bandwidth of the state-of-the-art time-domain measurement tools used [3]) which enables generating UWB signals with at least 70-GHz bandwidth. The enormous flexibility in the design of the coplanar network, which can be precisely implemented by highly accurate fabrication tools can enable a wideband randomly-shaped transfer function, resulting in a noise-like signal. In all of these potential examples, the system directly delivers the signal at large power levels, without the need for a post-amplification stage, which bypasses a major challenge in high-frequency electronics.

IV. Conclusion

This work revealed the potential of nanoplasma picosecond switches integrated with coplanar pulse-shaping networks for millimeter-wave and terahertz pulse generators and modulators in a single metal layer without a need for high-frequency amplifiers. The fabricated modulators provide large output powers (30 dBm) at high frequencies up to 66 GHz (limited by the bandwidth of the experimental setup). The ease of integration enables the implementation of the proposed concept on almost any platform, including flexible substrates, CMOS, and IIIV compounds. The proposed concept has relevance to future high-performance terahertz electronics.

REFERENCES

[1] L. Samoska, "An overview of solid-state integrated circuit amplifiers in the submillimeter-wave and THz regime," *IEEE Trans. Terahertz Sci. Technol.*, vol. 1, no. 1, pp. 9–24, Sep. 2011. doi: 10.1109/TTHZ.2011.2159558.

[2] D. Lee, A. Davydov, B. Mondal, G. Xiong, G. Morozov, and J. Kim, "From sub-terahertz to terahertz: challenges and design considerations," in 2020 *IEEE Wirel. Commun. and Networking Conf. Workshops*, IEEE, 2020, pp. 1–8. doi: 10.1109/WCNCW48565.2020.9124764.

[3] M. Samizadeh Nikoo, A. Jafari, N. Perera, M. Zhu, G. Santoruvo, and E. Matioli, "Nanoplasma-enabled picosecond switches for ultrafast electronics," *Nature*, vol. 579, no. 7800, pp. 534–539, Mar. 2020. doi: 10.1038/s41586-020-2118-y.

[4] L. Zhang, S. Liang, Y. Lv, D. Yang, X. Fu, X. Song, G. Gu, P. Xu, Y. Guo, A. Bu, et al., "High-power 300 ghz solid-state source chain based on gan doublers," *IEEE Electron Device Letters*, vol. 42, no. 11, pp. 1588–1591, 2021. doi: 10.1109/LED.2021.3110781.

[5] J. H. Hwang, K.-J. Lee, S.-M. Hong, and J.-H. Jang, "Balanced MSM-2DEG varactors based on AlGaN/GaN heterostructure with cutoff frequency of 1.54 THz," *IEEE Electron Device Letters*, vol. 38, no. 1, pp. 107–110, 2016. doi: 10.1109/LED.2016.2628866.

[6] M. Z. Win and R. A. Scholtz, "Impulse radio: How it works," *IEEE Commun. Lett.*, vol. 2, no. 2, pp. 36–38, Feb. 1998. doi: 10.1109/4234.660796.

[7] J. Zhang, P. Orlik, Z. Sahinoglu, A. F. Molisch, and P. Kinney, "UWB systems for wireless sensor networks," *Proc. IEEE* , vol. 97, no. 2, Feb. 2009. doi: 10.1109/JPROC.2008.2008786.

[8] E. Kaya and K. Entesari, "A CMOS microwave broadband adaptive dual-comb dielectric spectroscopy system for liquid chemical detection," in *Proc. IEEE/MTT-S Int. Microw. Symp.*, 2020, pp. 229–232. doi: 10.1109/IMS30576.2020.9223869.

[9] S. Razavian and A. Babakhani, "Silicon integrated THz comb radiator and receiver for broadband sensing and imaging applications," *IEEE Trans. Microw. Theory Techn.*, vol. 69, no. 11, 4937-4950 (2021). doi: 10.1109/TMTT.2021.3105436.

[10] F. S. Yamasaki, L. P. S. Neto, J. O. Rossi, and J. J. Barroso, "Soliton generation using nonlinear transmission lines," *IEEE Trans. Plasma Sci.*, vol. 42, no. 11, pp. 3471–3477, Nov. 2014. doi: 10.1109/TPS.2014.2361487.

[11] F. Khoeini, B. Hadidian, K. Zhang, and E. Afshari, "Reflection-based short pulse generation in CMOS," *IEEE Solid-State Circuits Lett.*, vol. 3, pp. 318–321, 2020. doi: 10.1109/LSSC.2020.3018129.

[12] M. Samizadeh Nikoo, A. Jafari, R. van Erp, and E. Matioli, "Kilowatt-range picosecond switching based on microplasma devices," *IEEE Electron Device Lett.*, vol. 42, no. 5, pp. 767-770, May. 2021. doi: 10.1109/LED.2021.3068732.

[13] L. Ye, K. Yuan, C. Zhu, Y. Zhang, Y. Zhang, K. Lai, "Broadband high-efficiency near-infrared graphene phase modulators enabled by metal–nanoribbon integrated hybrid plasmonic waveguides," *Nanophoton.*, vol. 11, no. 3, pp. 613-23, Jan. 2022. doi: 10.1515/nanoph-2021-0709.

[14] L. F. Ye, K. H. Sui, Y. Zhang, and Q. H. Liu, "Broadband optical waveguide modulators based on strongly coupled hybrid graphene and metal nanoribbons for near-infrared applications," *Nanoscale*, vol. 11, pp. 3229–3239, 2019. doi: 10.1039/C8NR09157A.

[15] Z. Liu, X. Zhu, W. Hu, and F. Jiang, "Principles of chaotic signal radar," *Int. J. Bifurcation Chaos*, vol. 17, no. 5, pp. 1735–1739, May 2007. doi: 10.1142/S0218127407018038.

[16] H. Mosalam, A. Allam, H. Jia, A. B. Abdel-Rahman, and R. K. Pokharel, "High efficiency and small group delay variations 0.18-µm CMOS UWB power amplifier," *IEEE Trans. Circuits Syst. II, Exp. Briefs*, vol. 66, no. 4, pp. 592–596, Apr. 2019. doi: 10.1109/TCSII.2018.2870165.

[17] M. G. M. Hussain, "Ultra-wideband impulse radar—An overview of the principles," *IEEE Aerosp. Electron. Syst. Mag.*, vol. 13, no. 9, pp. 9–14, 1998. doi: 10.1109/62.715515.

[18] W. Shao, A. Edalati, T. R. McCollough, and W. J. McCollough, "A timedomain measurement system for UWB microwave imaging," *IEEE Trans. Microw. Theory Techn.*, vol. 66, no. 5, pp. 2265–2275, May 2018. doi: 10.1109/TMTT.2018.2801862.

[19] E. Kaya and K. Entesari, "Silicon Integrated Broadband Dual Frequency Comb-based Microwave Detector for Material Characterization," in *Proc. IEEE Radio and Wireless Symp.*, 2022, pp. 229–232. doi: 10.1109/RWS53089.2022.9719944.

[20] C.-W. Hsue, L.-C. Tsai, and K.-L. Chen, "Implementation of first-order and second-order microwave differentiators," *IEEE Trans. Microw. Theory Tech.*, vol. 52, no. 5, pp. 1443–1448, May 2004. doi: 10.1109/TMTT.2004.827015.